Environ Sci Pollut Res (2016) 23:17982–17994
DOI 10.1007/s11356-016-6985-6

RESEARCH ARTICLE

Solar-driven photocatalytic treatment of diclofenac using immobilized TiO_2-based zeolite composites

Marin Kovacic[1] · Subhan Salaeh[1] · Hrvoje Kusic[1] · Andraz Suligoj[2,3] · Marko Kete[2] · Mattia Fanetti[4] · Urska Lavrencic Stangar[2] · Dionysios D. Dionysiou[5] · Ana Loncaric Bozic[1]

Received: 5 April 2016 / Accepted: 25 May 2016 / Published online: 3 June 2016

Abstract The study is aimed at evaluating the potential of immobilized TiO_2-based zeolite composite for solar-driven photocatalytic water treatment. In that purpose, TiO_2-iron-exchanged zeolite (FeZ) composite was prepared using commercial Aeroxide TiO_2 P25 and iron-exchanged zeolite of ZSM5 type, FeZ. The activity of TiO_2-FeZ, immobilized on glass support, was evaluated under solar irradiation for removal of diclofenac (DCF) in water. TiO_2-FeZ immobilized in a form of thin film was characterized for its morphology, structure, and composition using scanning electron microscopy/energy-dispersive x-ray spectroscopy (SEM/EDX). Diffuse reflectance spectroscopy (DRS) was used to determine potential changes in band gaps of prepared TiO_2-FeZ in comparison to pure TiO_2. The influence of pH, concentration of hydrogen peroxide, FeZ wt% within the composite, and photocatalyst dosage on DCF removal and conversion efficiency by solar/TiO_2-FeZ/H_2O_2 process was investigated. TiO_2-FeZ demonstrated higher photocatalytic activity than pure TiO_2 under solar irradiation in acidic conditions and presence of H_2O_2.

Keywords Photocatalysis · Thin films · TiO_2-FeZ · Solar irradiation · Diclofenac · Water treatment

Responsible editor: Suresh Pillai

Electronic supplementary material The online version of this article (doi:10.1007/s11356-016-6985-6) contains supplementary material, which is available to authorized users.

✉ Hrvoje Kusic
hkusic@fkit.hr

✉ Ana Loncaric Bozic
abozic@fkit.hr

[1] Faculty of Chemical Engineering and Technology, University of Zagreb, Marulicev trg 19, HR-10000 Zagreb, Croatia

[2] Laboratory for Environmental Research, University of Nova Gorica, Vipavska 13, SI-5000 Nova Gorica, Slovenia

[3] Laboratory for Inorganic Chemistry and Technology, National Institute of Chemistry, Hajdrihova 19, SI-1001 Ljubljana, Slovenia

[4] Materials Research Laboratory, University of Nova Gorica, Vipavska 11c, SI-5270 Ajdovscina, Slovenia

[5] Environmental Engineering and Science Program, University of Cincinnati, Cincinnati, OH 45221-0012, USA

Introduction

Heterogeneous photocatalysis employing semiconductor nanoparticles has shown to be an efficient technology for degrading a variety of recalcitrant organics into readily biodegradable products, and eventually mineralizing them to carbon dioxide and water. Wide application of nano-TiO_2 in photocatalytic water treatment gained significant interest due to high photocatalytic activity under the incident photon wavelength of <390 nm, as well as chemical and thermal stability (Chong et al., 2010; Fujishima et al., 2008; Ibhadon and Fitzpatrick, 2013; Pichat, 2013; Robertson et al., 2012; Schneider et al., 2014). However, a real-scale application of nano-TiO_2 in water treatment is facing challenges related to separation of nanoparticles after water treatment and their agglomeration during the operation of the process. A further technical challenge is associated with the limitation of TiO_2 to absorb irradiation energy in broader incident radiation range (Chong et al., 2010; Ibhadon and Fitzpatrick, 2013; Pelaez et al., 2012; Schneider et al., 2014). The latter can be improved through several strategies such as doping with non-metals, incorporation or deposition of noble metals (ions), as well as material engineering solutions based on composites formation using: transition metals, carbon nanotubes, dyed sensitizers, conductive polymers, and semiconducting

materials (Chong et al., 2010; Fagan et al., 2016; Ibhadon and Fitzpatrick, 2013; Pelaez et al., 2012). These solutions offer an attractive and energy-efficient option, utilizing the vast abundance of solar irradiation for catalyst activation, thus leading to a significant decrease of operational costs (Chong et al., 2010; Fagan et al., 2016; Pelaez et al., 2012). Immobilizing the photocatalysts on various supports, the in-treatment agglomeration and post-treatment separation issues can be overcome (Chong et al., 2010; Kete et al., 2014; Schneider et al., 2014).

In this work, we addressed the above-mentioned constrains of nano-TiO_2 photocatalysis by developing an immobilized TiO_2-iron-exchanged zeolite (FeZ) composite made of commercial Aeroxide TiO_2 P25 with FeZ. It is anticipated that the formation of TiO–O–Fe bonds would yield lower band gap and improved activity of composite material in comparison to Aeroxide TiO_2 P25 under solar irradiation (Lai et al., 2015; Liu et al., 2011). The coupling of TiO_2 with FeZ, as a microporous material, may increase the surface area and porosity of thin films, facilitating the generation of radical species (Fujishima et al., 2008; Noorjahan et al., 2004). Fenton catalytic cycle can be initiated by the addition of H_2O_2, providing an additional source of radical species within the photocatalytic system. The activity of as-prepared TiO_2-FeZ thin films under solar irradiation was tested on diclofenac (DCF) aqueous solution. DCF is one of the most widely available non-steroidal anti-inflammatory drugs which arrive in natural environment mainly from urine and feces as well as from the direct discharge of unused drugs into wastewater. The conventional municipal wastewater treatment plants are found to be insufficiently effective in the removal of DCF and other micropollutants. It has been shown that DCF may cause adverse effects to human health and the environment, especially in combination with other pharmaceuticals (Calza et al., 2006; Perez-Estrada et al., 2005A). DCF has recently been included in the first "watch list" of priority substances in water regulated by EU Water Framework Directive (EU, 2013). Accordingly, DCF is selected as a model pollutant to test the potential of advanced treatment technology, relying on a composite photocatalyst activated by solar irradiation. Within the study, TiO_2-FeZ thin films were characterized for morphology and composition. The influence of operational parameters of solar/TiO_2-FeZ/H_2O_2 was examined in order to enlighten the process chemistry and occurring phenomena. In that purpose, a statistical/empirical approach combining Box–Behnken experimental design (BBD) with response surface methodology (RSM) was employed.

Materials and methods

Chemicals

Diclofenac sodium salt ($C_{14}H_{10}Cl_2NNaO_2$, p.a., Sigma-Aldrich) was used as a model pollutant. As mobile phases for high-performance liquid chromatography (HPLC) methanol (CH_3OH, HPLC grade) and ortho-phosphoric acid (*o*-H_3PO_4, w≈85 %), both Sigma-Aldrich, were used. Ethanol (CH_3CH_2OH, abs., Sigma-Aldrich); titanium tetraisopropoxide (TTIP, $Ti\{OCH(CH_3)_2\}_4$, 97 %, Sigma-Aldrich); perchloric acid ($HClO_4$, 70 %, Kemika); tetraethyl orthosilicate (TEOS, $Si(OC_2H_5)_4$), 99 % GC grade, Sigma-Aldrich); hydrochloric acid (HCl, 36.5 %, Gram-mol); and Levasil® 200/30 (colloidal SiO_2, Obermeier) were used for preparation of thin films. Aeroxide TiO_2 P25 (Evonik); ZSM5-type zeolite (CVB8014, Zeolyst International); and ferrous sulfate ($FeSO_4 \times 7H_2O$, p.a., Kemika, Croatia) were used for photocatalyst preparation. Hydrogen peroxide (H_2O_2, $w = 30$ %, Gram-mol) was used as an oxidant in treatment process, while HCl and sodium hydroxide (NaOH, p.a., Kemika) were used for pH adjustment.

Photocatalysts preparation and immobilization

FeZ was prepared by solid-state ion exchange starting from NH_4ZSM5 zeolite applying the modified procedure of Rauscher et al. (1999), as referred in Juretic Perisic et al. (2016). Composite photocatalyst was prepared with different mass ratios TiO_2/FeZ wt%; 95:5, 72.5:27.5, and 50:50, hereinafter referred as TiO_2-FeZ-(5), TiO_2-FeZ-(27.5), and TiO_2-FeZ-(50), respectively, for the convenience of description. Such prepared powders were immobilized on glass plates ($r = 37.5$ mm) (ESM 1: Fig. S1, Supplementary materials), applying the procedure described in Kete et al. (2014), by spin coating (1500 rpm) technique using KW-4A Spin Coater, Chemat Technology, USA. Thin films of analogue TiO_2-NH_4ZSM5, and pure TiO_2 were prepared using the same procedure.

Photocatalysts activity under solar irradiation

The photocatalytic activity of thin films under solar irradiation was tested on the DCF solution ($c_0 = 0.1$ mM) in a water-jacketed ($V = 0.09$ L and $T = 25.0 \pm 0.2$ °C) batch photoreactor. The reactor was placed under the simulated solar irradiation source Oriel Arc source (Newport, USA) equipped with Xe lamp of 450 W (Osram, Germany). The used apparatus was equipped with an Oriel AM1.5 G air mass filter, correcting the output of arc lamp to approximate the solar spectrum when the sun is at a zenith angle of 48.2°. The light intensity was measured to be 124.78 ± 0.11 mW cm^{-2} using pyranometer CMP21 (Kipp & Zonen, Netherlands). The experimental procedure applied in DCF removal by solar/TiO_2-FeZ/H_2O_2 process was as follows. The pH of DCF water solution was adjusted at the desired value and then glass plates with TiO_2-FeZ thin films were placed at the bottom of the reactor. The reaction solution was then spiked with the required H_2O_2 aliquot. The mixing of solution was ensured with orbital shaker DOS-

20 (90 rpm, Neo-lab, Germany). Adsorption equilibrium was reached within 30 min in the dark, and thereafter, the reaction solution was exposed to the simulated solar irradiation. During experiments, 500-μL aliquots were taken at −30 (30 min prior to irradiation), 0 (starting of irradiation), 15, 30, 45, and 60 min, filtered using Chromafil XTRA RC (25 mm, 0.45 μm, Macherey Nagel, Germany), quenched with MeOH and submitted to HPLC analysis. In desorption tests, used plates were immersed in DI water (90 mL, pH 8.00 ± 0.05) and placed in shaker for 30 min; the samples were prepared for HPLC analysis according to the above-mentioned procedure.

Analyses

DCF concentration was monitored by HPLC, Series 10 (Shimadzu, Japan) equipped with UV-DAD, SPD-M10A_{VP} (Shimadzu, Japan) using XTerra MS C18 column (5 μm, 25.0 cm × 4.6 mm, Waters USA), and mobile phase CH_3OH/phosphate buffer operating at 1.0 mL min^{-1} flow. pH measurements were performed by Handylab pH/LF portable pH meter (Schott Instruments GmbH, Germany). UV/VIS spectrophotometer Lambda EZ 201 (PerkinElmer, USA) was used for the quantification of ferric iron by thiocyanate colorimetric method (Clesceri et al., 1998).

Diffuse reflectance spectra (DRS) of TiO_2 and TiO_2-FeZ thin films were measured using UV–Vis spectrophotometer equipped with an integrating sphere, Lambda 650S (PerkinElmer, USA). Band gaps were calculated on the basis of the reflectance vs. wavelength spectra, transformed into Kubelka–Munk function (K) vs. photon energy (hν) (Koci et al., 2009). The morphology of the prepared thin films was examined by scanning electron microscopy (SEM) using JSM7001 TTLS (JEOL, Japan) equipped with an energy-dispersive x-ray spectroscopy (EDXS) detector.

Calculations

The influence of pH, concentration of H_2O_2, and wt% of FeZ within the TiO_2-FeZ composite on the effectiveness of solar/TiO_2-FeZ/H_2O_2 process was screened by means of RSM. The values of aforementioned process parameters were transferred into the dimensionless coded values and represented by independent variables: X_1, X_2, and X_3 (Table 1). The experimental space, covering the ranges of studied parameters and their combinations, was described using Box–Behnken design (BBD) for solar/TiO_2-FeZ/H_2O_2 (ESM 1: Table S1, Supplementary Material) and 3^2 full factorial design (FFD) for solar/TiO_2/H_2O_2 (ESM 1: Table S2, Supplementary Material). The chosen processes responses were DCF removal (Y_1 and Y_3) and conversion (Y_2 and Y_4). The combined influence of studied parameters on process performance is described by quadratic polynomial equation representing RSM models (Myers et al., 2009). The obtained results and values of chosen responses are given in ESM 1: Tables S1 and S2 (Supplementary Material), for solar/TiO_2-FeZ/H_2O_2 and solar/TiO_2/H_2O_2, respectively. The fitting of RSM models was evaluated by coefficient of determination (R^2) and the analysis of variance (ANOVA), using STATISTICA 12.7, StatSoft and Dell; Design-Expert 10.0, StatEase; and Mathematica 10.0, Wolfram Research.

Table 1 Experimental range and levels of independent variables for solar/TiO_2-FeZSM5/H_2O_2 process

Process parameters	Model variables/ coded values	Level/range		
		−1	0	1
pH	X_1	4	5.5	7
[H_2O_2] (mM)	X_2	0.5	2.75	5
w(TiO_2)/w(FeZSM5) (%)	X_3	95:5	72.5:27.5	50:50

Results and discussion

Photocatalyst characterization

Our previous study (Juretic Perisic et al., 2016) revealed that used zeolite preserved its morphology upon solid-state ion exchange. Figure 1 presents SEM micrograph and EDX maps analysis of sample TiO_2-FeZ-(27.5). In Fig. 1a, the zeolite particles are visible (some of them are indicated by arrows), showing size about 1 μm. Figure 1b presents a high magnification image of a zeolite particle (red circle) embedded in the TiO_2–SiO_2 film. It can be seen that TiO_2 particles size ranges from 20 to 30 nm. In Fig. 1d–f, the EDX maps of Ti Lα, Si kα, and Fe Lα are shown, respectively. These EDX maps were acquired on the area represented in Fig. 1c. As shown, the layer is cracked and inhomogeneous, presumably as a consequence of differences in sizes of particles present in the thin film. TiO_2 particles are nano sized, while FeZ particles are micro sized (Evonik 2016; Juretic Perisic et al., 2016). The observed cracks in thin film layer might also be a consequence of compressive stresses due to heat treatment performed to achieve effective film fixation. As shown in Fig. 1d, e, TiO_2 and SiO_2 are dispersed rather evenly through the immobilized thin film. The brighter areas in the Si map (Fig. 1e) corresponds to zeolite particles or small zeolite clusters. According to our observation, zeolite is quite uniformly distributed and well dispersed within the films, without occurrence of major agglomeration. The Fe map (Fig. 1f) shows a different distribution, quite uncorrelated with zeolite distribution observed in Si map (Fig. 1e). Figure 1f reveals that the present Fe-rich clusters do not completely overlap with the location of zeolites. In general, Fe is observed to be mostly

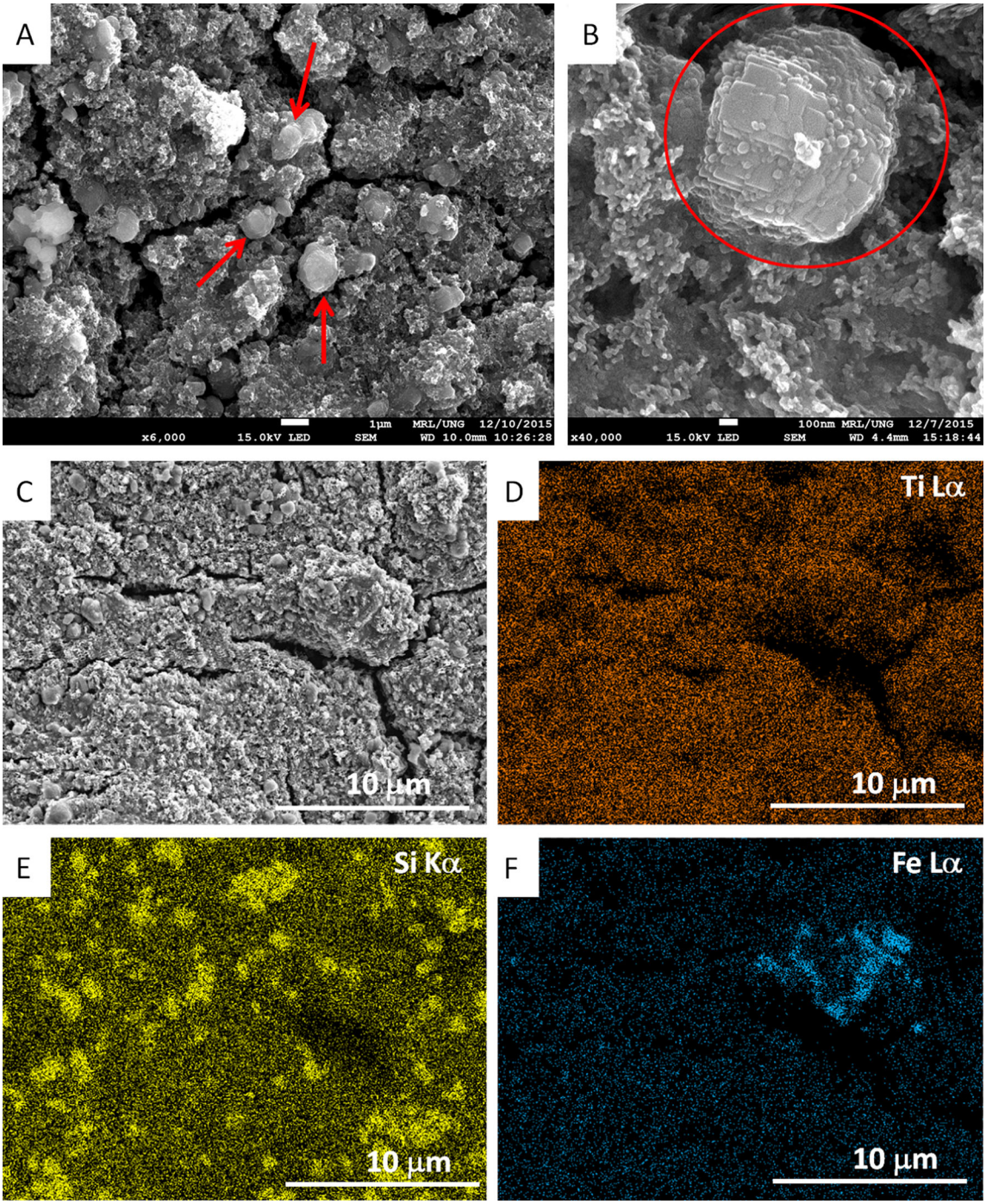

Fig. 1 SEM (**a**–**c**) and EDX maps of Ti (**d**), Si (**e**), and Fe (**f**) acquired on sample TiO_2-FeZ-(27.5)

agglomerated in separate clusters. The Fe Lα line intensity in spectra acquired out of those clusters (not shown) is very low, in some cases below the detectability limits (defined as $N_{bkg} + 3\text{sqrt}(N_{bkg})$, being N_{bkg} the counts of the background signal) in other cases slightly above, with an evaluated concentration of 0.4 ± 0.3 wt%. Similar scenario is observed on the two other samples with different zeolite concentration (5 and 50 %). In summary, SEM/EDX analysis indicates that zeolite is well dispersed in the film, while Fe is mostly agglomerated in separate clusters. The concentration of Fe out of these clusters is lower than the expected average (1.04 % in TiO_2-FeZ-(27.5)), which is close to the detection limit of the applied method.

DRS analysis of immobilized TiO_2 and TiO_2-FeZ composite photocatalysts thin films is presented in ESM 1: Fig. S2a (Supplementary material). The corresponding band gaps, calculated from Kubelka–Munk function (*K*) vs. photon energy (hν) (ESM 1: Fig. S2b, Supplementary material), follow a

decreasing order: TiO_2 (3.047) > TiO_2-FeZ-(5) (3.023) > TiO_2-FeZ-(27.5) (2.956) > TiO_2-FeZ-(50) (2.889). Such results are in accordance with the hypothesis that coupling of TiO_2 with transition metals would lead to lower band gaps (Chong et al., 2010; Pelaez et al., 2012; Liu et al., 2011) due to visible light-driven transfer of charge carries through the Ti–O–Fe heterojunction. An increase of FeZ wt% results in increase of iron content in the immobilized composite layer. Despite the noticed inhomogeneity of the thin films (Fig. 1), lowering of the band gaps is linearly correlated with the increase of the FeZ wt% in the composite.

The results of the characterization of immobilized TiO_2-FeZ composite photocatalyst, despite the observed inhomogeneity, indicate its potentially higher activity under solar irradiation in comparison to pure TiO_2, which was further investigated in the study.

Composite photocatalyst activity under solar irradiation

Preliminary tests of TiO_2-FeZ photoactivity were performed at pH values 4 and 7 and concentration of H_2O_2 of 0.5 and 5 mM. The bottom boundary was set to pH 4 in order to avoid the inconsistency of results due to the possible precipitation of DCF during oxidation experiments (Perez-Estrada et al., 2005b), although pH≈3 is stated in the literature as optimal for Fenton reaction (Chen and Pignatello, 1997; Esplugas et al., 2002; Jung et al., 2009; Tarr, 2003). The activity of TiO_2-FeZ-(27.5) toward DCF removal was compared with its analogue composite with pristine zeolite (NH_4ZSM5) and with pure TiO_2 (Fig. 2). In experiments performed at pH 4, TiO_2-FeZ showed similar (with lower [H_2O_2]) or somewhat better (with higher [H_2O_2]) effectiveness in DCF removal in comparison to pure TiO_2 (Fig. 2a, c, respectively). On the other hand, at neutral pH, DCF removal obtained by TiO_2-FeZ was significantly lower (with lower [H_2O_2]) or similar (with higher [H_2O_2]) comparing to pure TiO_2 (Fig. 2b, d, respectively). It can be seen that results obtained after the initial period in the dark differ significantly regarding the pH, but not so much regarding the photocatalyst composition and [H_2O_2]. Since photocatalytic degradation is favored when adsorption of present organics occurs (Chong et al., 2010; Pichat, 2013; Zhao et al., 2014), the much higher DCF removal obtained at lower pH, where the adsorption of DCF after 30-min dark period took place ((Fig. 2a, c, respectively), is logical. It should be noted that the composite made with pristine zeolite (NH_4ZSM5) showed lower effectiveness in comparison to pure TiO_2 in all cases, i.e., regardless of pH and [H_2O_2] (Fig. 2). Taking into account that the applied zeolite is not photoactive, as demonstrated in the previous studies (Kusic et al., 2006; Peternel et al., 2007), the results obtained in the case of TiO_2-NH_4ZSM5 composite are not surprising. The inclusion of NH_4ZSM5 into the composite, 27.5 wt% of photoactive compound (TiO_2) was replaced by inactive material, obviously causing the lowering of photocatalytic activity. Although the presence of microporous materials such as ZSM5 zeolite may increase the porosity of immobilized thin films (Fujishima et al., 2008; Noorjahan et al., 2004), this benefit most probably did not come to forth in the case of one-layered thin films. On the other hand, TiO_2-FeZ showed similar or better activity regarding DCF removal in comparison to TiO_2; the exception was the case at neutral pH and lower [H_2O_2], which yielded similar activity as that of the composite with pristine zeolite (NH_4ZSM5). Taking into account the already described potential benefits of FeZ within the composite and the obtained results presented in ESM 1: Fig. S2 (Supplementary material) and Fig. 2, we can conclude that in the case of TiO_2-FeZ, the presence of iron may be beneficial to the rates of oxidation in the system, due to Fenton reaction occurring in the presence of H_2O_2. The Fenton reaction requires acidic pH (Tarr, 2003), and accordingly, the results obtained at pH 4 suggest in favor of this oxidative mechanism as an addition to the photocatalytic degradation of DCF. The differences obtained in the cases with lower and higher [H_2O_2] at pH 4 suggest in favor of the assumed Fenton mechanism contributing to the overall system effectiveness. On the other hand, the calculated band gaps suggest the formation of Ti–O–Fe bond, providing higher activity of composite photocatalyst under solar radiation in comparison to pure TiO_2. This can be supported with similar DCF removal obtained by TiO_2 and TiO_2-FeZ composite at higher [H_2O_2] and pH 7, whereas the contribution of Fenton mechanism can be neglected.

Influence of process parameters on effectiveness of solar/TiO_2-FeZ/H_2O_2

The influence of parameters of solar/TiO_2-FeZ/H_2O_2 process such as pH, [H_2O_2], and wt% of FeZ within the composite on DCF removal and conversion were investigated using the RSM approach. The same was performed in the case of solar/TiO_2/H_2O_2, but with the exception of photocatalyst composition, in order to be used as a background for the process using TiO_2-FeZ. The fourth studied process parameter, the mass of the photocatalyst, was studied through the number of immobilized thin film layers. However, this action was not performed using RSM due to the fact that layer numbers would be presented as categorical parameter in the applied experimental design, significantly and unnecessarily increasing the number of experiments. Hence, the influence of layer number was studied at conditions determined as optimal by the applied RSM.

As mentioned above, BBD was used to navigate through the desired experimental range of process parameters influencing solar/TiO_2-FeZ/H_2O_2 process effectiveness in terms of DCF removal and conversion. In order to compare the process using TiO_2-FeZ composite photocatalyst, the

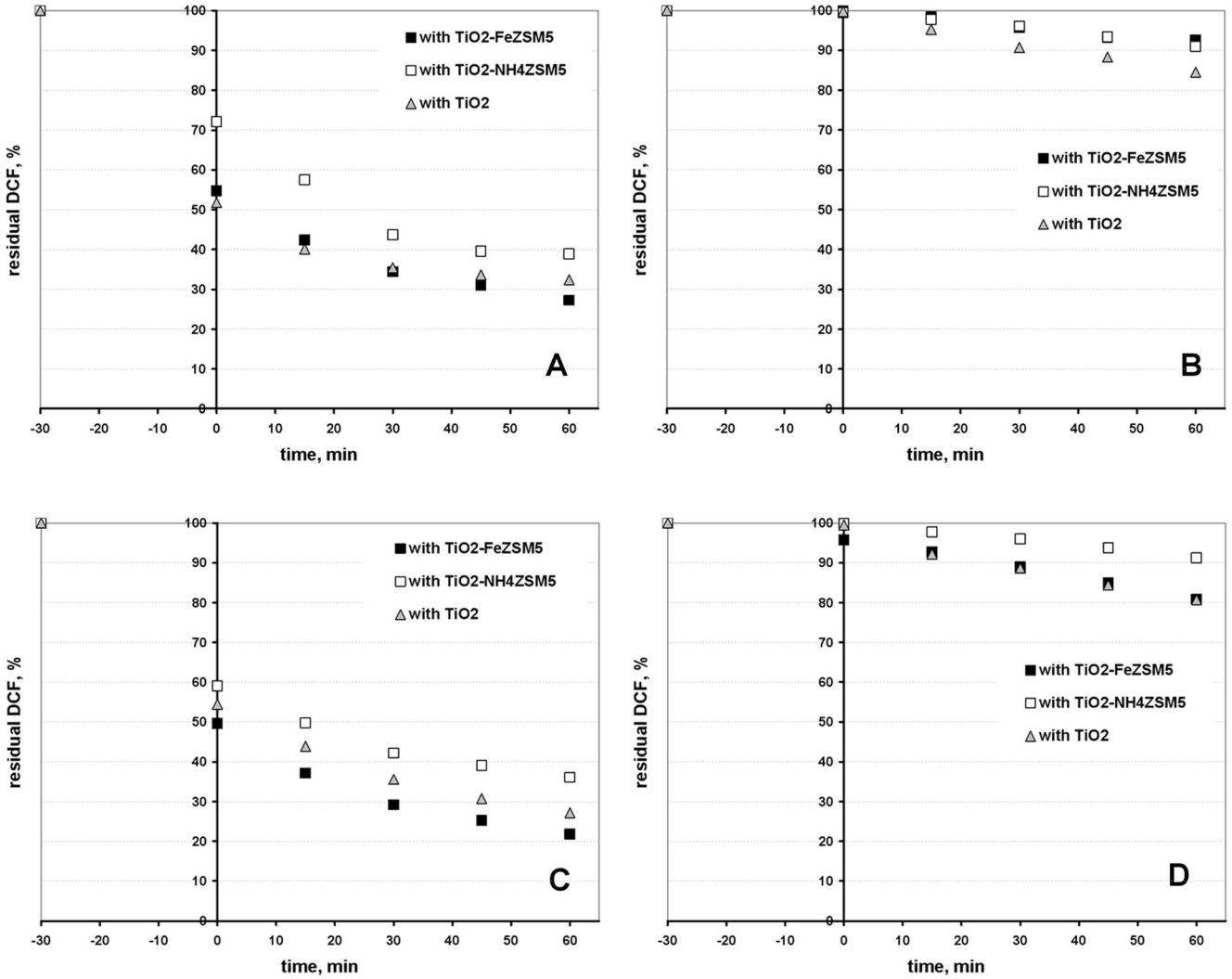

Fig. 2 Activity of immobilized photocatalysts TiO_2-FeZ-(27.5), TiO_2-NH_4ZSM5-(27.5), and TiO_2 in combination with H_2O_2 under solar radiation for DCF removal. **a** pH 4 and $[H_2O_2] = 0.5$ mM. **b** pH 7 and $[H_2O_2] = 0.5$ mM. **c** pH 4 and $[H_2O_2] = 5$ mM. **d** pH 7 and $[H_2O_2] = 5$ mM

analogues control treatment was performed using pure TiO_2 as a background. Here, FFD was used to establish the experimental matrix of process parameters (pH and $[H_2O_2]$) within the same range as in the case of TiO_2-FeZ. The BBD and FFD matrices are summarized in ESM 1: Tables S1 and S2, respectively (Supplementary Material), along with the obtained DCF removal and conversion extents after 60 min of exposure to the simulated solar irradiation, which were used as system responses. These tables also contain the corresponding responses predicted by RSM models M1–M4 for DCF removal and conversion obtained by solar/TiO_2-FeZ/H_2O_2 and solar/TiO_2/H_2O_2, respectively. DCF removal and conversion were monitored and separately modeled in order to obtain insights in the contribution of oxidative activity of applied photocatalysts in overall process efficiency. DCF removal was monitored by HPLC analysis of water samples collected periodically during the experiment, made of 30 min of a dark period in order to achieve equilibrium adsorption and 60 min under exposure to solar irradiation. The DCF conversion was calculated by subtracting the adsorbed portion which remained at the immobilized photocatalyst after the treatment from overall DCF removal. For each of the process responses (Y_1 and Y_3; removal, and Y_2 and Y_4; conversion) and for each photocatalyst type (TiO_2-FeZ and TiO_2), RSM models M1–M4 were derived by applying the multiple regression analysis on BBD or FFD matrices and corresponding experimental results. The model equations are listed in ESM 1: Table S3 (Supplementary material). By applying RSM modeling to get insight in the influence of the process parameters of the photocatalytic treatment misleading information that might be obtained using "one-parameter-at-the-time" approach would be avoided (Chong et al., 2010). In order to successfully apply RSM for intended actions, the first postulate is to have accurate, significant, and predictive models. Usually, RSM models are evaluated on the basis of analysis of variance (ANOVA), an essential test providing a list of statistical parameters such

as: Fisher F test value (F), its probability value (p), regression coefficients (pure; R^2, adjusted; R_{adj}^2, predicted; R_{pre}^2), t test value, etc. Most commonly, initial screening of model significance and accuracy may be provided through pertaining p, R^2, and R_{adj}^2 values (Debnath et al., 2015; Dopar et al., 2011; Myers et al., 2009; Yetilmezsoy et al., 2009). M1–M4 models derived in the study have been found to be significant (all having $p < 0.0001$; ESM 1: Tables S4 and S5, Supplementary Material), and accurate ($0.995 < R^2 < 0.999$ and $0.987 < R_{adj}^2 < 0.998$). The further judgment of RSM models accuracy, i.e., adequacy of model fitting to empirical values and corresponding lack of fit, includes the so-called residual diagnostic (RD), which is based on normal probability test, Levene's test, and constant variance test. Hence, RD for RSM M1–M4 models revealed that: (i) there are no violations in the assumptions that errors are normally distributed and independent of each other, (ii) the error variances are homogeneous, and (iii) residuals are independent, while the demonstration of performed graphical analysis of RD is given in ESM 1: Fig. S3 (Supplementary Material) for M1. Taking into account the above-given information on RSM M1–M4 models, it can be easily concluded that they can be used hereinafter as a tool to enlighten the influence of studied parameters on treatment effectiveness, and provide more information on occurring mechanisms, process chemistry, and benefits of TiO_2-FeZ over TiO_2.

The influential process parameters on treatment performance can be easily established through developed M1–M4 models taking into account their values of the statistical parameter p, summarized for each model term in ANOVA tables (ESM 1: Tables S4 and S5, Supplementary Material). The extent of its influence can not be estimated on p values alone, but using the Pareto chart, this can be easily determined, along with the potential antagonistic or synergistic nature toward process response (Fig. 2 and ESM 1: S4, Supplementary Material).

It can be easily concluded that the most influential parameter on the effectiveness of solar/TiO_2-FeZ/H_2O_2 process for removal and conversion of DCF is pH (Fig. 3). The standardized effects of corresponding model terms (X_1 and X_1^2) are 10 and 5 times higher than those of other statistically significant model terms X_3^2 and X_2, corresponding to FeZ wt% in composite and [H_2O_2], respectively. Similar results are obtained for the background process with pure TiO_2 (ESM 1: Fig. S4, Supplementary Material). The findings of RSM modeling on our composite photocatalyst, applied within solar/TiO_2-FeZ/H_2O_2 process, are in accordance with the importance of pH in both photocatalytic- and Fenton-type processes. Namely, the operating pH predominantly influences the photocatalyst surface charge, which is responsible for its ability to adsorb organic contaminants (Chong et al., 2010). One of the postulates for the effective degradation of organics by photocatalytic treatment is their adsorption on the catalyst surface where they

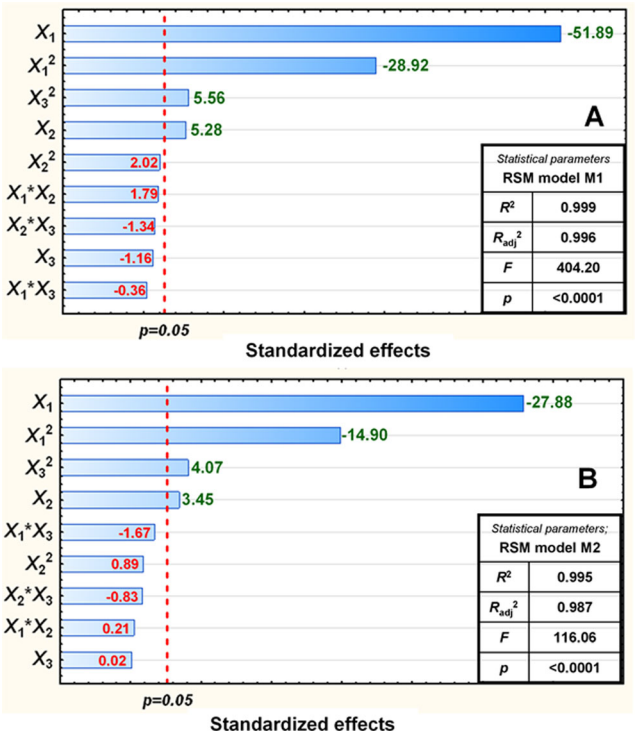

Fig. 3 Pareto chart representing the standardized effect of independent variables (studied process parameters) and their interactions on DCF removal (**a**) and conversion (**b**) by solar/TiO_2-FeZ/H_2O_2 process

can be degraded directly on photogenerated holes (h^+) or indirectly by formed reactive oxygenated species (ROS, predominately HO• and O_2•$^-$) at catalyst surface, overcoming mass transfer limitations related to their diffusion into the solution (Pichat, 2013; Robertson et al., 2012). Furthermore, in the presence of H_2O_2, TiO_2-FeZ can act as heterogeneous Fenton-type catalysts. It is well known that Fenton reaction is favored at pH values near 3 (Chen and Pignatello, 1997; Esplugas et al., 2002; Jung et al., 2009; Tarr, 2003). At pH values higher than 4.5, Fenton catalysts would become ineffective, due to the formation of stable ferri–hydroxide complexes (Dopar et al., 2011; Tarr, 2003). However, at a pH range between 2.5 to 4.5, the photoactive complex $Fe^{III}(OH)^{2+}$ would prevail, which may cause the formation of HO• under solar irradiation (Dopar et al., 2011; Nadtochenko and Kiwi, 1998). As shown in our previous study (Juretic Perisic et al., 2016), FeZ has the ability to adsorb DCF via complexation of deprotonated DCF ethanoic group with surface iron, which occurs at acidic pH (≤5). The degradation of such complexes can be effectively initiated by UV-A irradiation. Taking into account the physico-chemical phenomena related with pH and applied TiO_2-FeZ and its constituents, it is clear that effective DCF removal and consequent degradation would highly be pH dependent. Many authors reported the importance to maintain the photocatalytic reactions below the catalyst's point of zero charge (PZC) (Chong et al., 2010). The literature values of pH_{PZC} for

Aeroxide TiO_2 P25 range from 6.5 to 6.7 (Boncagni et al., 2009; Buscio et al., 2015; Kritikos et al., 2007). However, pH_{PZC} values of FeZ and pristine NH_4ZSM5 are found to be 2.37 and 2.81, respectively (Juretic Perisic et al., 2016). Hence, the surface charge and corresponding adsorption effect would be in relationship with TiO_2/FeZ ratio in applied composite photocatalyst, which would also determine DCF adsorption via iron-complexation mentioned earlier. As can be seen from Table 1, summarizing tested range of solar/TiO_2-FeZ/H_2O_2 process considered within BBD matrix, all experiments were performed above pH_{PZC} value of FeZ, but mostly below pH_{PZC} value of TiO_2. Hence, it can be concluded that DCF would be adsorbed by TiO_2 at pH 4 and 5.5, but not at pH 7. Besides, FeZ would be able to adsorb DCF via iron-complexation at pH 4, but not at higher pH. The effect of adsorption, which occurred within 30 min in the dark, is clearly demonstrated in Fig. 2 for pH values 4 and 7. In order to demonstrate the role of FeZ and its wt% in the composite photocatalyst in adsorption of DCF, we compared DCF removal by solar/TiO_2-FeZ/H_2O_2 and analogues process using TiO_2-NH_4ZSM5 composite through applied BBD. The results are shown in Fig. 4, while comparison of kinetics profiles for DCF removal is given in ESM 1: Fig. S5 (Supplementary Material). As can be seen, only in experiments #1, #3, #5, and #7 (ESM 1: Table S1, Supplementary Material), which were performed at pH 4, a noticeable DCF removal was obtained after 30 min of the dark period (Fig. 4a). These experiments yield noticeable DCF conversions as well (Fig. 4b). Similar DCF removal, regardless of composite type, was obtained after dark period only in the case of experiment #5 (TiO_2 present in 95 wt%), while in other experiments performed at pH 4, the adsorbed amount of DCF by TiO_2-FeZ was higher for 10 to 17 % comparing to TiO_2-NH_4ZSM5 (Fig. 4a). Such results support the above-stated importance of FeZ in the adsorption of DCF at acidic conditions.

Although model terms corresponding to [H_2O_2] and FeZ wt% in composite showed significantly lower contributions to the end point, i.e., process responses DCF removal and conversion, they are still significant (Fig. 3). Moreover, the ratio of their standard effects and those of model terms corresponding to pH is lower in the case of DCF conversion (1:4.5 and 1:7.5, Fig. 3b) in comparison to those obtained for DCF removal (1:5 and 1:10, Fig. 3a).

The influence of [H_2O_2] on DCF removal, but even more on DCF conversion, can be considered through both potential mechanisms for forming ROS: photocatalytic (1) and Fenton (2) (Pichat, 2013; Tarr, 2003):

$$H_2O_2 + H^+ + e^- \rightarrow HO\bullet + H_2O \quad (1)$$

$$Fe^{2+} + H_2O_2 \rightarrow Fe^{3+} + HO\bullet + HO^- \quad (2)$$

The presence of H_2O_2 in the photocatalytic process would result, besides the reaction of H_2O_2 with photogenerated electrons (e^-) (1), in the efficient suppression of back e^-/h^+ recombination, leading to higher efficiency of forming HO• through reaction (3) (Pichat, 2013):

$$H_2O + h^+ \rightarrow HO\bullet + H^+ \quad (3)$$

Hence, photocatalytic system would yield higher effectiveness due to the above-mentioned combined effect. On the other hand, the role of H_2O_2 in Fenton reaction is well known (Tarr, 2003); while the above-given primary reaction of Fenton catalytic cycle describing HO• formation can be considered to occur in our system as sequential upon illumination of photoactive complex $Fe^{III}(OH)^{2+}$ (4), prevailing in the pH range 2.5 to 4.5 (Dopar et al., 2011), due to the fact that FeZ contain ferric iron (Juretic Perisic et al., 2016):

$$Fe^{III}(OH)^{2+} \xrightarrow{h\nu} Fe^{2+} + HO\bullet \quad (4)$$

Besides, an additional amount of HO• is formed through reaction (4). It should be pointed out that all the above-given mechanisms of forming ROS through the involvement of H_2O_2 prefer acidic conditions, additionally supporting the importance of pH, which is found to be the most significant process parameter (Fig. 3). As standardized effects of both model terms corresponding to pH have negative indexes, providing antagonistic effect toward DCF removal and conversion, i.e., favoring acidic pH, the discussed role of H_2O_2 is in accordance with the found positive index of its standardized effect (Fig. 3), and in such manner, provided synergistic effect toward process response.

The significance of FeZ wt% in composite is reflected through its role to act as a heterogeneous Fenton-type catalyst at acidic pH (as described earlier), but also as a contributor of transition metals (Fe) in the system which may result with the formation of TiO–O–Fe bonds, yielding lower band gaps. The latter is demonstrated through DRS analysis, where an increase of FeZ within the composite was linearly correlated with the lower band gap values (ESM 1: Fig. S2, Supplementary Material). Hence, higher FeZ wt% sets the basis for the composite photocatalyst to be more active under solar irradiation in comparison to pure TiO_2. However, it should be noted that ZSM5-type zeolite is not a photoactive compound as TiO_2 (as demonstrated in Fig. 2). The presence of iron (as FeZ) may be advantageous through the photoactive component $Fe^{III}(OH)^{2+}$. Therefore, a positive effect might be expected with the increase of FeZ wt% in the composite, which is in accordance with the positive index of standard effect corresponding to its model term (Fig. 3).

The above-explained influences of studied parameters of solar/TiO_2-FeZ/H_2O_2 process, as well as their mutual interactions, can be clearly seen from 3D graphs (Fig. 5). The top row (Fig. 5a–c) refers to DCF removal, while the bottom row refers to DCF conversion. As can be seen from Figs. 5a and

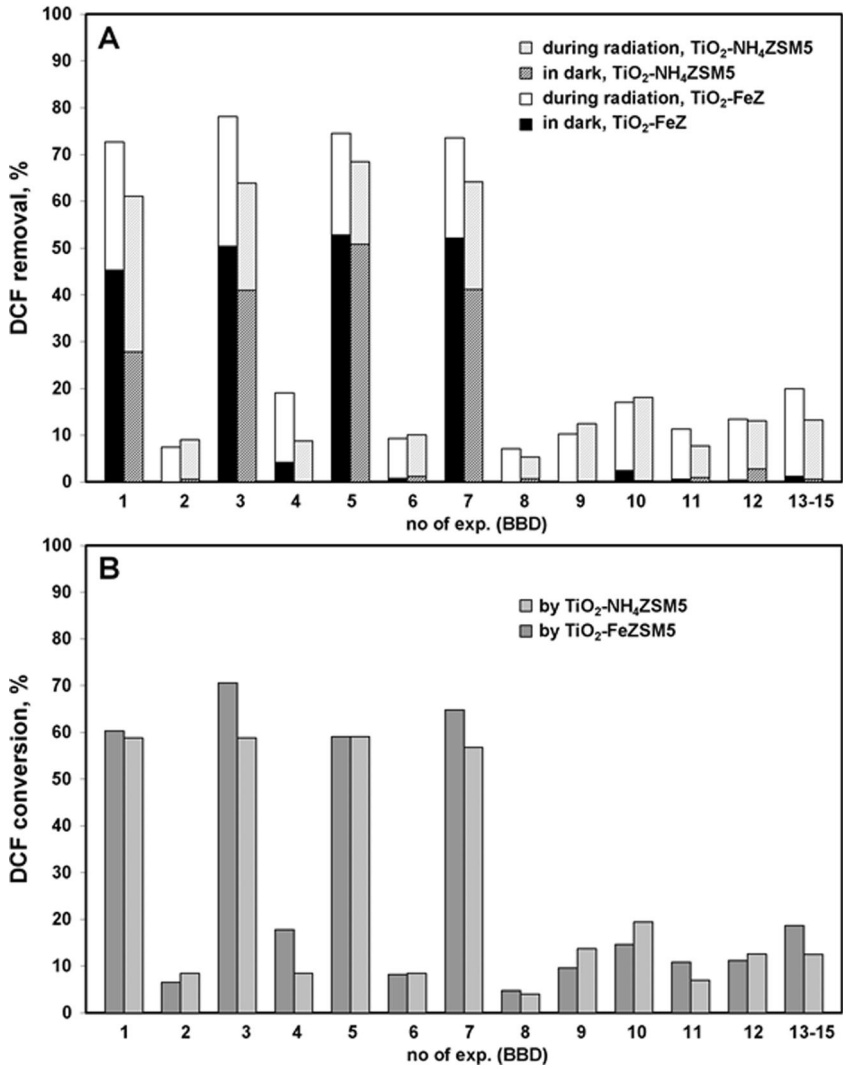

Fig. 4 Comparison of DCF removal (**a**) and conversion (**b**) using TiO_2-FeZ and TiO_2-NH_4ZSM5 in combination with H_2O_2 under solar radiation at conditions set by BBD (ESM 1: Table S1, Supplementary material)

6b, d, e, the presented mutual interactions of pH and [H_2O_2], and pH and FeZ wt% in the composite, toward DCF removal and conversion, have shown the indisputable dominant influence of pH. Since similar layouts were obtained for DCF removal and conversion, it might be concluded that degradation mechanism included adsorption of DCF onto TiO_2-FeZ due to its positive surface charge and complexation with surface iron, facilitating the degradation at catalysts surface upon illumination by solar irradiation. Consequently, significantly lower conversion extents were obtained in the cases where the adsorption of DCF was weak; only negligible differences between removal and conversion were obtained (Fig. 4. and ESM 1: Table S1, supplementary material). The portion of DCF removed, but not converted to by-products, ranged from 0.60 to 15.47 % of initial DCF in the system. The highest values of removed, but unconverted DCF were obtained at pH 4 (exp. #1, #3, #5, and #7; ESM 1: Table S1, Supplementary material). However, in the same experiments, the highest conversion extents were obtained, ranging from 59.1 to 70.6 % (Fig. 4b). As can be seen from Fig. 5, pH and [H_2O_2] have a clear antagonistic and synergistic effect, respectively, toward DCF removal and conversion. However, the effect of FeZ wt% in the composite was twofold. The increase of FeZ in the composite showed positive effect up to a certain point, where further increase resulted in lower DCF removal (Fig. 5b, c) and conversion (Fig. 5e, f). Among tested composites, TiO_2-FeZ-(50) has the lowest band gap, which was assumed to be accompanied by the highest activity under solar irradiation. However, this was not supported by the results obtained. The plausible explanation can be found in the combined photocatalytic and Fenton mechanisms involved in degradation of DCF, as explained earlier.

The background process with pure TiO_2 and solar/TiO_2/H_2O_2, showed a similar 3D graph for mutual interactions between pH and [H_2O_2] (Fig. 6) as obtained for solar/TiO_2-FeZ/H_2O_2 process with TiO_2-FeZ-(27.5) (Fig. 5a, d). This result supports the above-stated importance of pH for photocatalytic processes, manifested through the change of surface charge

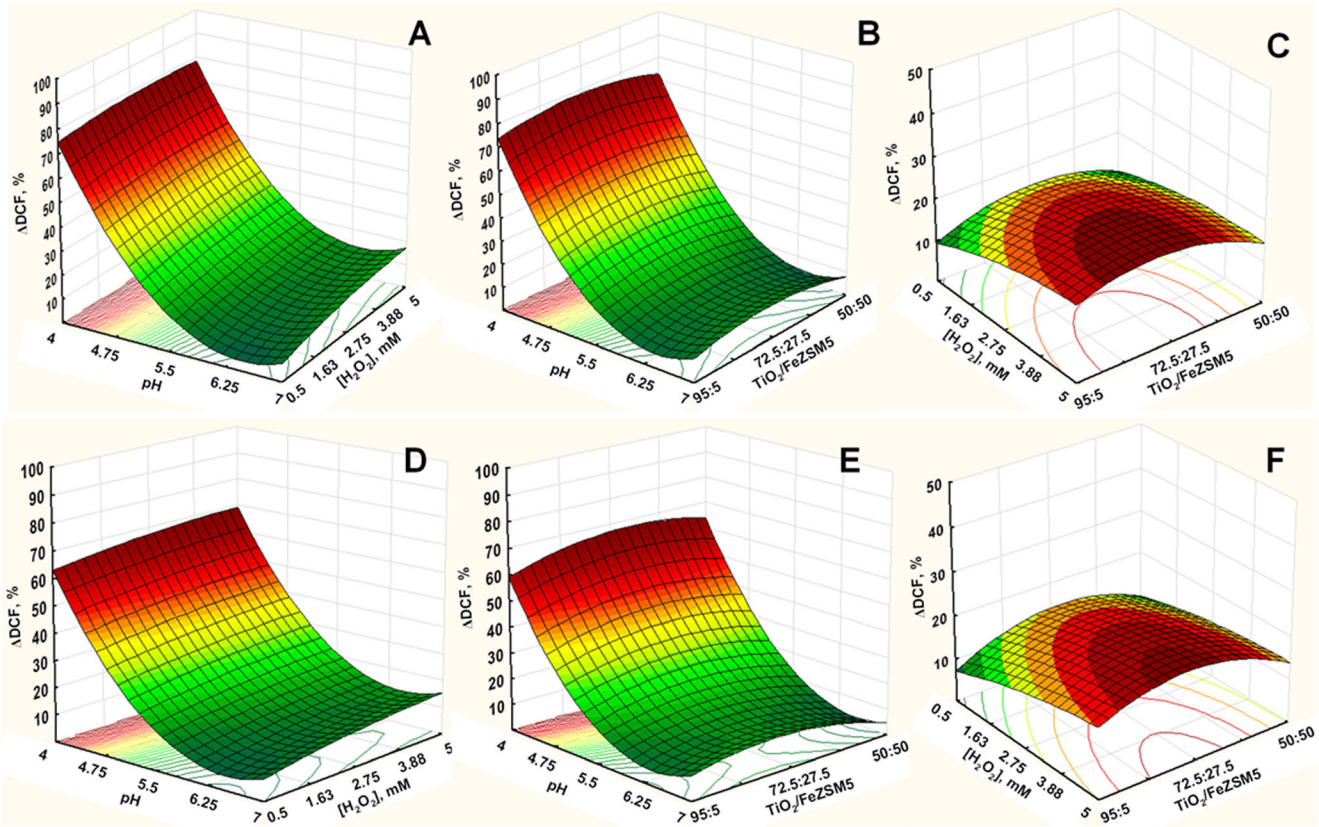

Fig. 5 3D response surface and contour diagrams showing the effects of the mutual interactions of initial pH and $[H_2O_2]$ **a** and **d**, pH and TiO_2/FeZ ratio **b** and **e**, and $[H_2O_2]$ and TiO_2/FeZ ratio **c** and **f** on the DCF removal (*top row*) and conversion (*bottom row*) by solar/TiO_2-FeZ/H_2O_2 process (TiO_2/FeZ ratio, $[H_2O_2]$, and pH were held at their respective center levels (**a** and **d**, **b** and **e**, and **c** and **f**, respectively)

and causing consequent adsorption of organics and their sequential degradation at the catalyst surface. However, the overall effectiveness of background process with TiO_2 at acidic conditions was lower for 5–10 % than that obtained by solar/TiO_2-FeZ/H_2O_2 process, speaking in favor of TiO_2-FeZ as more effective, presumably due to mentioned higher activity under solar irradiation and Fenton mechanism.

In order to evaluate the influence of the amount of photocatalyst, represented through the number of immobilized thin film layers, the optimal conditions for the highest removal of DCF by solar/TiO_2-FeZ/H_2O_2 and solar/TiO_2/H_2O_2 process were determined by finding the extreme values of RSM models M1 and M3. These models were used due to the fact that DCF removal is a precondition for effective DCF conversion. Besides, as it is pointed out, the influence of process parameters studied was almost identical in the case of DCF removal and conversion. It was found out that maximal DCF removal predicted by RSM model M1, 78.6 %, by solar/TiO_2-

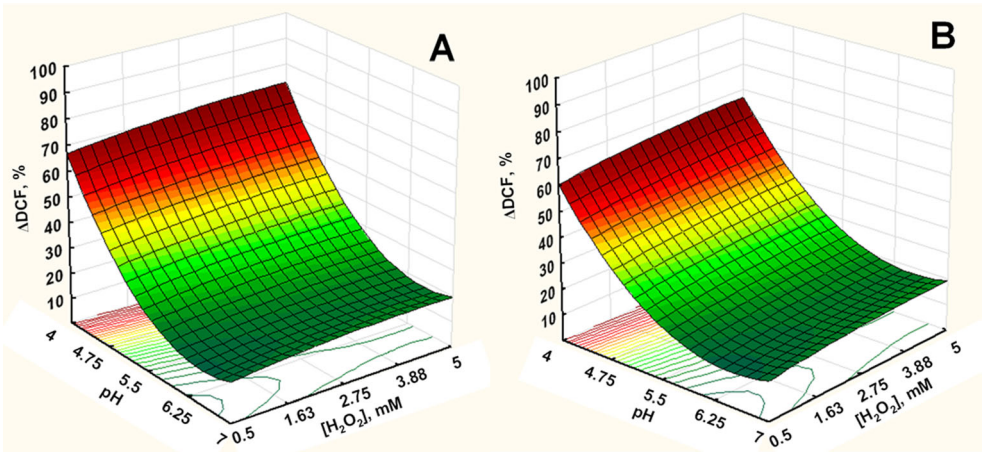

Fig. 6 3D response surface and contour diagrams showing the effects of the mutual interactions of initial pH and $[H_2O_2]$ on the DCF removal (**a**) and conversion (**b**) by solar/TiO_2/H_2O_2 process

FeZ/H_2O_2 process would be obtained at pH 4, $[H_2O_2] = 3.86$ mM and 25.4 wt% of FeZ within the composite. Similar conditions were found for the background case with pure TiO_2, solar/TiO_2/H_2O_2 process; pH 4 and $[H_2O_2] = 5.0$ mM for 72.5 % DCF removal. The experiments with 1–5 thin film layers of TiO_2-FeZ and pure TiO_2 were performed at these conditions. The kinetic results are shown in Fig. 7, while Fig. 8 summarize DCF removal and conversion, as well as results of thin film stability toward attrition after the treatment. As can be seen, 78.3 and 72.8 % of DCF removals were obtained by solar/TiO_2-FeZ/H_2O_2 and solar/TiO_2/H_2O_2 processes, respectively, using one layer of immobilized photocatalysts (Figs. 7 and 8). The results are very close to those predicted by RSM models M1 and M3 (78.6 and 72.5 %, respectively), additionally speaking in favor of their validity and accuracy. An increase of TiO_2-FeZ dosage (represented through an increased number of thin film layers) showed positive effect toward DCF removal, accomplished either during 30 min in the dark or overall after the treatment (Figs. 7a and 8a). However, the adsorption ability of composite catalyst in the dark increased for 3–4.5 % by increasing the layer numbers from 1 to 4 (55.0, 59.5, 62.7, and 66.4 %), while significant improvement was achieved with five layers (for approx. 15 %; up to 81.8 %) (Fig. 7a). On the other hand, the more significant improvement in overall DCF removal due to the increase of TiO_2-FeZ dosage was achieved with four and five layers, 88.8 and 91.8 %, respectively (Figs. 7a and 8a). As can be seen, the background process with pure TiO_2 did not show pronounced differences as a consequence of the increase of TiO_2 dosage through layers numbers from 1 to 5; the adsorption in dark increased from 45.6 to 53.5 %, while overall removal from 72.8 to 80.9 % (Fig. 7b). Similar results, i.e., the improvement regarding the number of thin film layers and photocatalyst type, can be observed for DCF conversion (Fig. 8.). The catalyst dosage in photocatalytic water treatment was determined to be one of the crucial parameters; it affects the overall photocatalytic reaction rate (Chong et al., 2010; Ibhadon and Fitzpatrick, 2013). In a suspension process, the

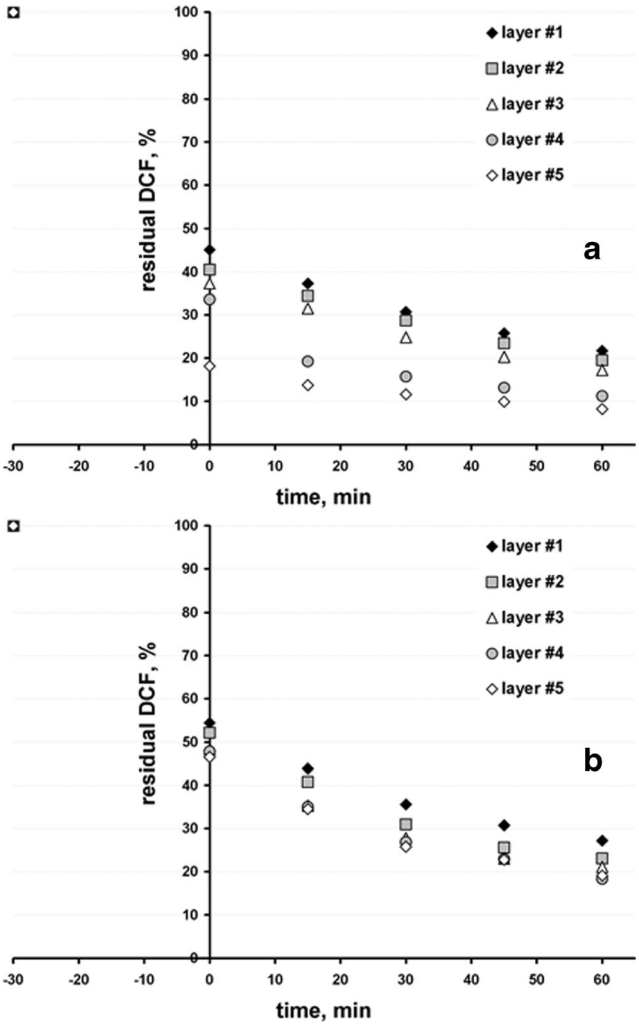

Fig. 7 DCF removal kinetics by (**a**) solar/TiO_2-FeZ/H_2O_2 (pH 4, $[H_2O_2] = 3.86$ mM, w(TiO_2):w(FeZ) = 74.6:25.4) and (**b**) solar/TiO_2/H_2O_2 processes (pH 4, $[H_2O_2] = 5$ mM) depending on the catalyst dosage (represented through number of thin film layers with immobilized catalyst)

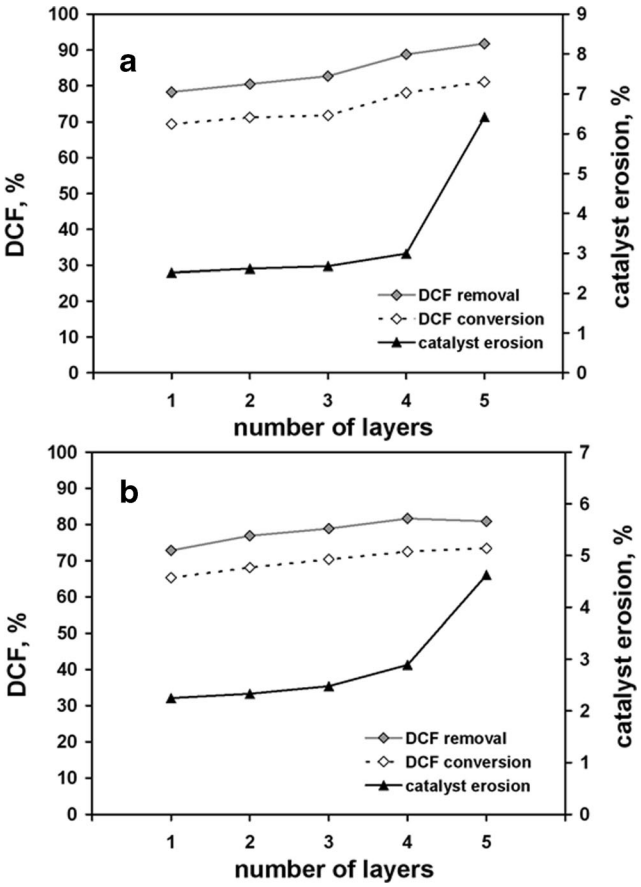

Fig. 8 DCF removal and conversion after 60-min treatment by (**a**) solar/TiO_2-FeZ/H_2O_2 (pH 4, $[H_2O_2] = 3.86$ mM, w(TiO_2):w(FeZ) = 74.6:25.4) and (**b**) solar/TiO_2/H_2O_2 processes (pH 4, $[H_2O_2] = 5$ mM) depending on the catalyst dosage (represented through number of thin film layers with supported catalyst), including catalyst erosion data

catalyst dosage influences the reaction rate linearly almost up to achievement of the saturation level, where catalyst dosage significantly influences the light photon absorption due to increased turbidity in the system. This effect is also a function of reactor geometry and working conditions. Systems operated in the suspension mode are usually characterized with better mass transfer (due to higher uniformity of contact between the catalyst and organic pollutant), which is one of the major issues of system operated with immobilized catalyst (Chong et al., 2010). However, in such a system mode, the agglomeration of catalyst particles during treatment and the need for post-treatment separation are avoided (Ibhadon and Fitzpatrick, 2013; Pichat, 2013). Several features are important for systems with the immobilized catalysts; providing more effective mass transfer, depth of light penetration, and stability of immobilized catalyst toward attrition. Accordingly, the mixing of the DCF aqueous solution in order to provide a much better contact with the immobilized catalyst surface as possible, was accomplished using the shaker. Another potential solution, which involves the usage of a reactor with recirculation, was not shown as practical due to DCF affinity toward adsorption to all available flexible tubing tested (PVC, polypropylene, silicon, tygon®). The depth of light penetration is usually crucial for the solutions showing high affinity to absorb photons (e.g., organics highly absorb photons of emitted energy) or causing competition in photon absorption (e.g., colored solutions). This was not the limiting factor in our study, since the solution was transparent, while the DCF degradation solely by applied simulated solar source in the observed period (60 min) was negligible (less than 0.2 %; results not shown). The catalyst stability toward erosion was monitored, and as can be seen (Fig. 8), the thin film layers were rather stable up to four layers; only 2.7 % of the catalyst weight was lost due to erosion. More importantly, this loss was consistent, regardless of catalyst type (i.e., composite TiO_2-FeZ or pure TiO_2) and layer numbers, indicating that surface eroded just slightly. However, with five layers, more significant erosion occurred (more than 6.4 % in the case of TiO_2-FeZ), indicating that such a catalyst might not be highly effective through consecutive application. Hence, the case with TiO_2-FeZ with four layers was chosen as the most efficient, providing rather good of photocatalytic performance (i.e., DCF removal and conversion) and stability.

Conclusions

TiO_2-FeZ composite photocatalyst was successfully prepared in a form of thin film using commercial AEROXIDE TiO_2 P25 and iron-exchanged zeolite of ZSM5 type, FeZ. The activity of the immobilized TiO_2-FeZ under simulated solar light was tested and compared with pure TiO_2 in regard to their effectiveness for the removal and conversion of DCF.

The immobilized TiO_2-FeZ was inspected for its morphology, structure, and composition using SEM/EDX technique. The observed cracks and inhomogeneity are contributed to different sizes of particles present in the thin films and compressive stresses during the heat treatment. The band gaps of the prepared catalysts were determined using the data obtained through DRS analysis. The obtained results revealed that TiO_2-FeZ composition was preserved, resulting in a linear relationship between lowering of the band gap vs. FeZ wt% increase.

In the presence of H_2O_2 at acidic conditions, TiO_2-FeZ exhibited higher photocatalytic activity under solar irradiation in comparison to pure TiO_2. On the other hand, pure TiO_2 was more effective at neutral conditions. RSM approach was applied to investigate the influence of solar/TiO_2-FeZ/H_2O_2 process parameters on the effectiveness of DCF removal and conversion. It was demonstrated that pH has a dominant role. The significance of [H_2O_2] and FeZ wt% content in the composite indicated the combined contribution of photocatalytic and Fenton mechanisms involved in DCF degradation. The photocatalyst dosage, studied through the increasing number of thin film layers, showed a positive effect toward DCF removal and conversion. The stability of immobilized thin films was preserved up to four layers.

Acknowledgement We acknowledge the financial support from the Croatian Science Foundation (Project UIP-11-2013-7900; *Environmental Implications of the Application of Nanomaterials in Water Purification Technologies* (*NanoWaP*)). We acknowledge Dr. Ivana Steinberg for providing the laboratory equipment for spin coating. We acknowledge Dr. Davor Ljubas, Dr. Damir Dovic, and Alan Rodic, all from the Faculty of Mechanical Engineering and Naval Architecture, University of Zagreb, Croatia, for their contribution in light intensity measurements.

References

Boncagni NT, Otaegui JM, Warner E, Curran T, Ren J, Fidalgo de Cortalezzi MM (2009) Exchange of TiO_2 nanoparticles between streams and streambeds. Environ Sci Technol 43:7699–7705

Buscio V, Brosillon S, Mendret J, Crespi M, Gutiérrez-Bouzán C (2015) Photocatalytic membrane reactor for the removal of C.I. Disperse Red 73. Mater 8:3633–3647

Calza P, Sakkas VA, Medana C, Baiocchi C, Dimou A, Pelizzetti E, Albanis T (2006) Photocatalytic degradation study of diclofenac over aqueous TiO_2 suspensions. Appl Catal B 67:197–205

Chen R, Pignatello JJ (1997) Role of quinine intermediates as electron shuttles in Fenton and photoassisted Fenton oxidations of aromatic compounds. Environ Sci Technol 31:2399–2406

Chong MN, Jin B, Chow CWK, Saint C (2010) Recent developments in photocatalytic water treatment technology: a review. Water Res 44: 2997–3027

Clesceri LS, Greenberg AE, Eaton AD (1998) Standard methods for the examination of water and wastewater treatment, 20th edn. APHA & AWWA & WEF, USA

Debnath S, Ballav N, Nyoni H, Maity A, Pillay K (2015) Optimization and mechanism elucidation of the catalytic photo-degradation of the

dyes Eosin Yellow (EY) and Naphthol blue black (NBB) by a polyaniline-coated titanium dioxide nanocomposite. Appl Catal B 163:330–342

Dopar M, Kusic H, Koprivanac N (2011) Treatment of simulated industrial wastewater by photo-Fenton process: Part I. The optimization of process parameters using design of experiments (DOE). Chem Eng J 173:267–279

Esplugas S, Gimenez J, Contreras S, Pascual E, Rodriguez M (2002) Comparison of different advanced oxidation processes for phenol degradation. Water Res 36:1034–1042

EU (2013) Directive 2013/39/EU of the European Parliament and of the Council amending Directives 2000/60/EC and 2008/105/EC as regards priority substances in the field of water policy. Off J Eur Commun 226:1–17

Evonik Industries (2016) AEROXIDE®, AERODISP® and AEROPERL® Titanium Dioxide as photocatalyst, Technical information 1243 - Accessed on Feb 29, 2016. https://www.aerosil.com/sites/lists/IM/Documents/TI-1243-Titanium-Dioxide-as-Photocatalyst-EN.pdf

Fagan R, McCormack DE, Dionysiou DD, Pillai SC (2016) A review of solar and visible light active TiO_2 photocatalysis for treating bacteria, cyanotoxins and contaminants of emerging concern. Mat Sci Semicon Proc 42:2–14

Fujishima A, Zhang X, Tryk DA (2008) TiO_2 photocatalysis and related surface phenomena. Surf Sci Rep 63:515–582

Ibhadon AO, Fitzpatrick P (2013) Heterogeneous photocatalysis: recent advances and applications. Catalysts 3:189–218

Jung YS, Lim WT, Park J-Y, Kim Y-H (2009) Effect of pH on Fenton and Fenton-like oxidation. Environ Technol 30:183–190

Juretic Perisic D, Gilja V, Novak Stankov M, Katancic Z, Kusic H, Lavrencic Stangar U, Dionysiou DD, Loncaric Bozic A (2016) Removal of diclofenac from water by zeolite-assisted advanced oxidation processes. J Photochem Photobiol A 321:238–247

Kete M, Pavlica E, Fresno F, Bratina G, Lavrencic Stangar U (2014) Highly active photocatalytic coatings prepared by a low-temperature method. Environ Sci Poll Res 21:11238–11249

Koci K, Obalova L, Matejova L, Placha D, Lacny Z, Jirkovsky J, Solcova O (2009) Effect of TiO_2 particle size on the photocatalytic reduction of CO_2. Appl Catal B 89:494–502

Kritikos DE, Xekoukoulotakis NP, Psillakis E, Mantzavinos D (2007) Photocatalytic degradation of reactive black 5 in aqueous solutions: Effect of operating conditions and coupling with ultrasound irradiation. Water Res 41:2236–2246

Kusic H, Koprivanac N, Selanec I (2006) Fe-exchanged zeolite as the effective heterogeneous Fenton-type catalyst for the organic pollutant minimization: UV irradiation assistance. Chemosphere 65:65–73

Lai Y, Liu W, Fang J, Qin F, Wang M, Yu F, Zhang K (2015) Fe-doped anatase TiO_2/carbon composite as an anode with superior reversible capacity for lithium storage. RSC Adv 5:93676–93683

Liu Y, Wei JH, Xiong R, Pan CX, Shi J (2011) Enhanced visible light photocatalytic properties of Fe-doped TiO_2 nanorod clusters and monodispersed nanoparticles. Appl Surf Sci 257:8121–8126

Myers RH, Montgomery DC, Anderson-Cook CM (2009) Response surface methodology: process and product optimization using designed experiments, 3rd edn. Wiley, Hoboken

Nadtochenko VA, Kiwi J (1998) Photolysis of $FeOH^{2+}$ and $FeCl^{2+}$ in aqueous solution. Photodissociation kinetics and quantum yields. Inorg Chem 37:5233–5238

Noorjahan M, Durga Kumari V, Subrahmanyam M, Boule P (2004) A novel and efficient photocatalyst: TiO_2-HZSM-5 combinate thin film. Appl Catal B 47:209–213

Pelaez M, Nolan NT, Pillai SC, Seery MK, Falaras P, Kontos AG, Dunlop PSM, Hamilton JWJ, Byrne JA, O'Shea K, Entezari MH, Dionysiou DD (2012) A review on the visible light active titanium dioxide photocatalysts for environmental applications. Appl Catal B 125: 331–349

Perez-Estrada LA, Maldonado MI, Gernjak W, Aguera A, Fernandez-Alba AR, Ballesteros MM, Malato S (2005a) Decomposition of diclofenac by solar driven photocatalysis at pilot plant scale. Catal Today 101:219–226

Perez-Estrada LA, Malato S, Gernjak W, Aguera A, Thurman EM, Ferrer I, Fernandez-Alba AR (2005b) Photo-Fenton degradation of diclofenac: identification of main intermediates and degradation pathway. Environ Sci Technol 39:8300–8306

Peternel I, Koprivanac N, Loncaric Bozic A, Kusic H (2007) Comparative study of UV/TiO_2, UV/ZnO and UV/Fenton processes for the organic reactive dye in aqueous solution. J Hazard Mater 148:477–484

Pichat P (2013) Photocatalysis and water purification: from fundamentals to recent applications. Wiley, Weinheim

Rauscher M, Kesore K, Mönning R, Schwieger W, Tissler A, Turek T (1999) Preparation of a highly reactive FeZSM5 catalyst through solid-state ion exchange for the catalytic decomposition of N_2O. Appl Catal A 184:249–256

Robertson PKJ, Robertson JMC, Bahnemann DW (2012) Removal of microorganisms and their chemical metabolites from water using semiconductor photocatalysis. J Hazard Mater 211–212:161–171

Schneider J, Matsuoka M, Takeuchi M, Zhang J, Horiuchi Y, Anpo M, Bahnemann DW (2014) Understanding TiO_2 photocatalysis: mechanisms and materials. Chem Rev 114:9919–9986

Tarr MA (2003) Fenton and modified Fenton methods for pollutant degradation. In: Tarr MA (ed) Chemical degradation methods for wastes and pollutants—environmental and industrial applications. Marcel Dekker, Inc, New York, pp 165–200

Yetilmezsoy K, Demirel S, Vanderbei RJ (2009) Response surface modeling of Pb(II) removal from aqueous solution by Pistacia vera L.: Box-Behnken experimental design. J Hazard Mater 171:551–562

Zhao C, Pelaez M, Dionysiou DD, Pillai SC, Byrne JA, O'Shea KE (2014) UV and visible light activated TiO2 photocatalysis of 6-hydroxymethyl uracil, a model compound for the potent cyanotoxin cylindrospermopsin. Catal Today 224:70–76